



Catalytic decomposition of benzothiophenic and dibenzothiophenic sulfones over MgO-based catalysts



Ramanathan Sundararaman¹, Chunshan Song*

Clean Fuels and Catalysis Program, EMS Energy Institute and Department of Energy and Mineral Engineering, The Pennsylvania State University, 209 Academic Projects Bldg, University Park, PA 16802, USA

ARTICLE INFO

Article history:

Received 28 July 2013

Received in revised form

28 September 2013

Accepted 15 October 2013

Available online 23 October 2013

Keywords:

Oxidative desulfurization

Sulfone decomposition

MgO

Solid base catalysts

Hydrocarbon fuel

ABSTRACT

Bulk and supported MgO based catalysts with weight loadings from 3 to 30 wt% were prepared by wet impregnation (WI) and sol–gel (SG) methods and tested for sulfone decomposition to sulfur-free hydrocarbon in real and surrogate liquid hydrocarbon fuels. The catalysts were characterized by BET analysis, XRD measurements, CO₂–chemisorption and XPS. Among bulk MgO, MgO/Al₂O₃ (WI) and MgO/SiO₂ (WI) catalysts, activity for sulfone decomposition was greatly influenced by crystallite size of MgO. Increasing calcination temperature increased MgO crystallite size which adversely affected catalytic activity. 30MgO/SiO₂ (WI) showed the highest activity for decomposition of sulfones both in real jet and diesel fuels. The effect of temperature on decomposition of benzothiophenic and dibenzothiophenic sulfones over 30MgO/SiO₂ (WI) was examined from 320 to 450 °C using (pre-oxidized) JP-5 jet fuel and BP-325 diesel fuel to elucidate the difference in decomposition activity of two and three ring sulfones. At 450 °C, about 77% of the dibenzothiophenic sulfones in BP-325 diesel fuel were decomposed over 30MgO/SiO₂ catalysts. Benzothiophenic sulfones were more active for decomposition and about 97% of the sulfones in JP-5 jet fuel were decomposed at 400 °C. In contrast to bulk MgO, MgO/Al₂O₃ (WI) and MgO/SiO₂ (WI) catalysts; MgO/TiO₂ (WI) and MgO/SiO₂ (SG) promoted undesired conversion of sulfones back to sulfur compounds by oxygen removal. The difference in selectivity was attributed to the effect of support and synthesis procedure potentially resulting in catalyst with different surface properties. Model compounds decomposition of dibenzothiophenic sulfone and 3-methyl benzothiophene sulfone were also studied to evaluate the potential pathway from sulfones to sulfur-free hydrocarbons.

© 2013 Elsevier B.V. All rights reserved.

1. Introduction

The stringent sulfur regulation has motivated intensive research in non-conventional desulfurization techniques of liquid hydrocarbon fuels [1–3]. For example, oxidative desulfurization (ODS) has been extensively studied on diesel fuel because of the increased reactivity of alkylated dibenzothiophenes for oxidation which are hard to remove by conventional hydrodesulfurization (HDS) [4–11]. Unlike HDS, oxidation of sulfur compounds does not result in the formation of sulfur-free hydrocarbon and therefore requires post-oxidation steps for effective removal of oxidized sulfur compounds to yield low sulfur product.

Most studies on ODS have, however, focused on catalyst and oxidant development for selective oxidation [12–18] with fewer efforts on treatment of oxidized sulfur compounds or sulfones

obtained after oxidation [19–26]. By theory, sulfones can be easily extracted or adsorbed because of their increased polarity in comparison to the parent sulfur compounds. Although liquid extraction of sulfones by polar solvents is feasible and has been demonstrated, the loss of whole hydrocarbon containing the sulfone can be an issue. A study by Otsaki et al. quantified the loss of hydrocarbon in straight run gas oil and vacuum gas oil when the oxidized sulfur is extracted by polar solvents [25]. The authors showed that dimethyl formamide extraction of sulfones from oxidized vacuum gas oil (2.17 wt% S) to <0.1 wt% S results in 35% feed loss and requires multiple extraction steps [25]. Like extraction, adsorption can be used for removal of sulfones but rapid saturation of the bed and the need for regeneration of the sorbent are some of the limitations. Further disposition of the effluent containing sulfones after regeneration can be an issue.

To overcome the limitations involved with post-separation techniques based on adsorption and extraction, we report in this paper the decomposition of benzothiophenic and dibenzothiophenic sulfones to sulfur-free hydrocarbon using real and model hydrocarbon feeds in the presence of MgO-based catalysts. The potential reaction scheme of the decomposition process is presented in Fig. 1.

* Corresponding author. Tel.: +1 814 863 4466; fax: +1 814 865 3573.

E-mail addresses: csong@psu.edu, hoscxs@gmail.com (C. Song).

¹ Present address: ExxonMobil Research and Engineering Co., Annandale, NJ 08801, USA.

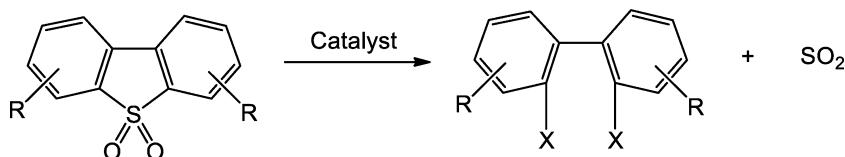


Fig. 1. Reaction scheme for catalytic decomposition of alkylated dibenzothiophenic sulfones (R: H or alkyl group, X: H or alkyl group from other hydrocarbons in the feed).

Decomposition of oxidized sulfur compounds using model compounds has been demonstrated in previous studies, but most of the efforts used large amounts of molten NaOH or KOH which are corrosive and tend to produce products of complex nature [27–29]. To avoid the limitations associated with NaOH based chemistry, heterogeneous catalysts have been proposed in some recent studies [19,20,30,31]. For example, Kocal and Brandvold postulated that decomposition of dibenzothiophene sulfone over heterogeneous catalyst results in the formation of hydroxybiphenyl and volatile sulfur compounds (sulfur dioxide) [26]. Heterogeneous NaOH based, sodium aluminate was shown to be effective for decomposition of sulfones in liquid hydrocarbon and addressed the handling issue of molten alkali by impregnating NaOH on alumina [31]. Even though heterogeneous system has been shown to be effective, the nature of the products obtained from decomposition of dibenzothiophenic sulfones is unknown. Also very limited work has been carried out on decomposition of benzothiophenic-type sulfones over heterogeneous catalysts.

This paper discusses the catalytic decomposition of benzothiophenic and dibenzothiophenic sulfones over a series of MgO based catalysts viz., MgO, MgO/SiO₂ prepared by sol–gel method, MgO/SiO₂, MgO/Al₂O₃ and MgO/TiO₂ catalysts prepared by wet impregnation procedure. Catalysts were characterized by BET, XRD, CO₂-chemisorption (TPD-MS and FTIR) and XPS to understand the influence of physical and chemical properties of the catalysts for decomposition of sulfones. Both real and surrogate liquid hydrocarbons containing different types of oxidized sulfur compounds were tested for sulfone decomposition chemistry.

2. Experimental

2.1. Catalysts synthesis and characterization

Catalyst used in this study were prepared by wet impregnation of magnesium ethoxide (98%, Sigma Aldrich) from its methanol solution onto γ -Al₂O₃ (UOP LaRoche VGL-15), fumed SiO₂ (Cabosil M5) and TiO₂ (Degussa P25) supports. A catalyst based on MgO/SiO₂ was also prepared by sol–gel method. A typical sol–gel synthesis involves premixing of magnesium ethoxide dissolved in methanol and tetraethyl orthosilicate (98%, Sigma Aldrich) in ethanol, followed by drop wise addition of water which results in the formation of a gel. The gel is then dried overnight at 80 °C followed by calcination at the desired temperature. Typical MgO loading of all the supported catalysts was 30 wt%. Unsupported MgO catalysts, MgO–ME (obtained by direct calcination of magnesium ethoxide) and MgO–SA obtained from Sigma Aldrich were also tested for their catalytic activity. All catalyst samples were calcined at the desired temperature between 450 and 650 °C for 5 h in a muffle furnace.

N₂ adsorption–desorption was carried out at liquid-N₂ temperature (–196 °C) to measure the BET (Brunauer–Emmett–Teller) surface area and pore volume on a Micromeritics ASAP 2020 analyzer. All samples were degassed at 200 °C under vacuum prior to measurement.

Temperature-programmed desorption of CO₂ (CO₂-TPD) was conducted in a flow mode on a Micromeritics Autochem 2910 TPR/TPD analyzer. In a typical CO₂-TPD experiment, about 150 mg of the sample was loaded in U-shaped quartz cell above a small

amount of quartz wool. The sample was dried under argon flow at 200 °C for 60 min. After the treatment, the temperature was cooled to 50 °C. CO₂ adsorption was facilitated by passing a 50% CO₂–helium mixture at 40 mL/min. After CO₂ adsorption, the CO₂-TPD profile of the sample was recorded by increasing the temperature from 50 to 900 °C at a heating rate of 10 °C/min under 50 mL/min of UHP He flow. The desorbed CO₂ was identified on the basis of the intensity of the mass fragment with *m/e* = 44 which was analyzed by AMETEK Dycor DM200M mass spectrometer.

Powder X-ray diffraction (XRD) patterns of the calcined catalysts were obtained on a Scintag (Thermo Scientific) PAD V Powder Diffractometer using Cu K α radiation (λ = 0.154 nm) operated at 30 mA and 35 kV with a scanning speed of 1°/min. The diffractograms were analyzed using MDI JADE 8.0 software and the standard JCPDS files.

Fourier transform infrared spectrometry (FTIR) was carried out on a Bruker Optics IFS 66/S equipped with diffuse reflectance IR Fourier transform spectrometry (DRIFTS), Thermo Spectra-Tech Collector II. The catalyst samples were analyzed using a micro sampling cup and all spectra were referenced to KBr. Samples were dried in-situ at 250 °C under a flow of argon at 40 mL/min and then temperature was reduced to 50 °C followed by exposure to CO₂ at 40 mL/min for analysis of type of basic sites of the catalyst. The spectra before and after CO₂ adsorption were recorded in diffuse reflectance model and the difference spectrum obtained was used for further analysis.

XPS analysis of the spent catalysts was performed on a Kratos Analytical Axis Ultra using a monochromatized Al K α X-ray source (1486.6 eV) at 280 W, with pass energy of 20 eV and a step size of 0.1 eV. Charge referencing of the features was done relative to the aliphatic carbon peak in C 1s spectrum at 285 eV. Spent catalysts were analyzed without any further treatment after sulfone decomposition reaction.

Spent catalyst from sulfone decomposition reaction were analyzed by thermogravimetric analysis on a TGA 2050 (TA Instruments) analyzer with argon and the sample was heated from room temperature to 1000 °C at 20 °C/min. Gaseous effluent from the TGA was analyzed by a ThermoStar GSD 301T mass spectrometer (Pfeiffer Vacuum Inc.).

2.2. Catalytic Reaction

The sulfone decomposition reactions were carried out in a downflow fixed-bed reactor at atmospheric pressure and temperatures between 320 and 450 °C with constant weight hourly space velocity (WHSV) of 10 h^{–1}. On top of the catalyst bed was a pre-heating zone, about 4 in. in length filled with glass beads of 2 mm in diameter. A high-pressure liquid chromatography pump was used to measure and pump the liquid hydrocarbon feedstock. A gas–liquid separator was employed to separate the reaction products into gas and liquid phases. The gaseous effluents were scrubbed in a basic solution before being vented out and were not analyzed in this study except in a few cases. Three K-type thermocouples were used to measure and maintain the temperature of the reactor unit. The first was used to measure the temperature of the tubular furnace and the second was placed on the outer wall of the reactor tube. The third thermocouple was placed at the center of

Table 1
Feedstocks sulfur content and flow reactor conditions.

Sulfur content of real fuels in ppmw		
Oxidized low sulfur diesel	350	
Oxidized JP-5 jet fuel	1050	
Model fuel composition		
Fuel containing dibenzothiophene sulfone	wt%	S, ppmw
tert-butyl benzene	41.8	
Tetrahydronaphthalene	19.1	
Cumene	11.9	
o-xylene	11.5	
Decane	15.9	
Dibenzothiophene sulfone		350
Fuel containing 3-methyl benzothiophene sulfone		
tri-isopropyl benzene	61.9	
tetrahydronaphthalene	19.3	
decane	15.8	
3-methyl benzothiophene sulfone		350
Sulfone decomposition reaction		
Temperature, °C	320 – 450	
Weight hourly space velocity, h ⁻¹	10	
Catalyst particle size, mm	0.5–1.0 (18–35 mesh)	
Catalyst weight, g	0.25	

the catalyst bed. All temperature measurements reported in this study were from the thermocouple placed in the catalyst bed.

The pre-oxidized JP-5-1050 jet fuel and pre-oxidized BP-325 diesel fuel were used as feeds for sulfone decomposition studies. A real JP-5 jet fuel (JP-5-1050) containing 1050 ppmw S and a low sulfur diesel (BP-325) containing 325 ppmw S were obtained from U.S. Office of Naval Research via Altex Technologies Corporation (Sunnyvale, California) and BP America, respectively. BP-325 diesel fuel was obtained from BP America in 2005 before ULSD regulations of having sulfur content of no more than 15 ppm was implemented starting June 2006. The obtained BP-325 diesel fuel was purged with nitrogen and sealed under an inert atmosphere to prevent undesired oxidation of the fuel during storage. For preparation of the real fuel samples, oxidation of sulfur compounds in the real jet and diesel fuels was carried out by using cumene hydroperoxide as an oxidant in the presence of 15% MoO₃/SiO₂ catalyst at 80 °C [12,13,14,15,16,17,18]. Oxidant to sulfur molar ratio was set at 20 and under the experimental conditions employed almost all sulfur compounds in jet and diesel fuels were oxidized, which was confirmed by analysis of fuel samples by GC equipped with PFPD (pulsed flame photometric detector). Two model feeds containing 350 ppmw S of 3-methyl benzothiophene sulfone and dibenzothiophene sulfone were prepared and tested for reaction mechanism studies. All catalytic tests were run at least for 4 h with maximum for 25 h. Model fuel properties and reaction conditions employed in this study are summarized in Table 1.

2.3. Hydrocarbon and sulfur analysis

The total sulfur concentration in real oxidized JP-5-1050 jet fuel and oxidized BP-325 diesel fuels was analyzed by using an Antek 9000 series total sulfur analyzer. Although sulfones generated by oxidation of sulfur compounds have less solubility because of their increased polarity, we did not observe any precipitation of sulfones in both oxidized JP-5-1050 jet fuel and oxidized BP-325 diesel fuels. This is consistent with our previous study on air oxidative desulfurization of real jet and diesel fuels where precipitation of sulfones was not observed in both jet (580 ppmw S) and diesel (41 ppmw S) fuels [7]. Analysis of aromatic content of jet and diesel fuels was not carried out in this study but it is expected that aromatics in diesel is less than 35% and less than 20% in jet fuel. The absence of solubility issue in jet fuel even in an aromatic lean condition shows that sulfones based on 2-ring aromatics might have better solubility. Also sulfur analysis of JP-5-1050 jet fuel and BP-325 diesel before and

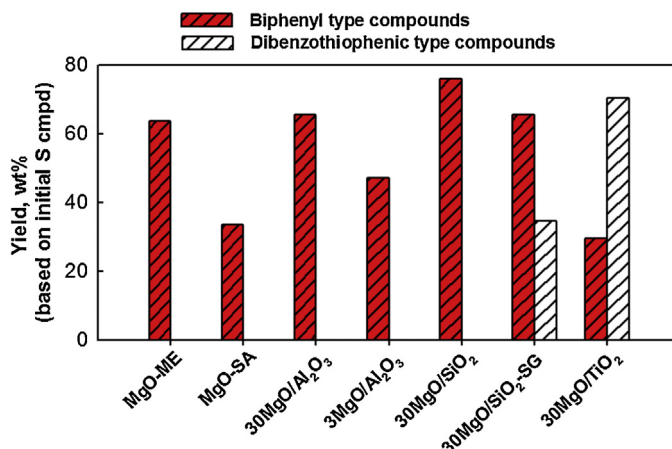


Fig. 2. Effect of support on activity of MgO based catalysts on decomposition of oxidized sulfur compounds in BP-325 diesel fuel [Reaction conditions: atm pressure; Temp, 450 °C; WHSV, 10 h⁻¹]. Catalytic activity were recorded at specific TOS (time on stream) of 4 h. All catalysts were calcined at 450 °C.

after oxidation did not show any significant difference in total sulfur concentration. Qualitative analysis of the sulfur compounds in real fuel was conducted with HP 5890 gas chromatograph (XTI-5 column from Restek, 30 m in length and 0.25 mm in internal diameter) equipped with a pulsed flame photometric detector (PFPD). The GC–MS was performed on a Shimadzu GC-174 coupled with a Shimadzu QP-5000 MS detector for identification of products from catalytic decomposition of sulfones in model feedstock.

3. Results and discussion

3.1. Catalytic activity of supported and bulkMgO samples

The catalysts were evaluated for activity in decomposition of sulfones in (pre-oxidized) BP-325 real diesel fuel at 450 °C and atmospheric pressure. All the catalysts were tested on an equal weight basis and were calcined at 450 °C in air before sulfone decomposition tests. The sulfone decomposition performances are presented in Fig. 2. Reference sample (bulk MgO-SA) obtained from Sigma Aldrich was also tested for catalytic performance. Catalytic activity presented in Fig. 2 were recorded at a specific TOS (time on stream) of 4 h for all catalyst samples.

For most of the samples including the reference material the major reaction observed was conversion of dibenzothiophenic sulfones to sulfur-free biphenyl type hydrocarbon. Apart from major reaction, the only undesired side reaction observed was conversion of dibenzothiophenic sulfones back to dibenzothiophene type sulfur compounds on 30MgO/SiO₂-SG and 30MgO/TiO₂ catalysts. This was confirmed by analysis of the product samples by GC-PFPD as shown in Fig. 3. The top chromatograph shows the dibenzothiophenic type sulfones that are present in the distillate sample which was used as the feed for the sulfone decomposition runs. About 65% and 29% of the dibenzothiophenic type sulfones are decomposed to biphenyl type compounds over 30MgO/SiO₂-SG and 30MgO/TiO₂ samples, respectively. But GC-PFPD analysis showed that the rest of the sulfones were converted back to dibenzothiophenic type compounds. About 35% of the sulfones were converted to parent dibenzothiophenic type compounds on 30MgO/SiO₂-SG catalyst prepared by sol gel procedure. It has been reported that mixed oxide of MgO and SiO₂ containing 25–30% MgO can have high concentrations of acid centers which can be weakly or moderately acidic [32]. This acidic nature can potentially contribute to deoxygenation of sulfones in the distillate to dibenzothiophenic type sulfur compounds. This observation is consistent with our earlier findings

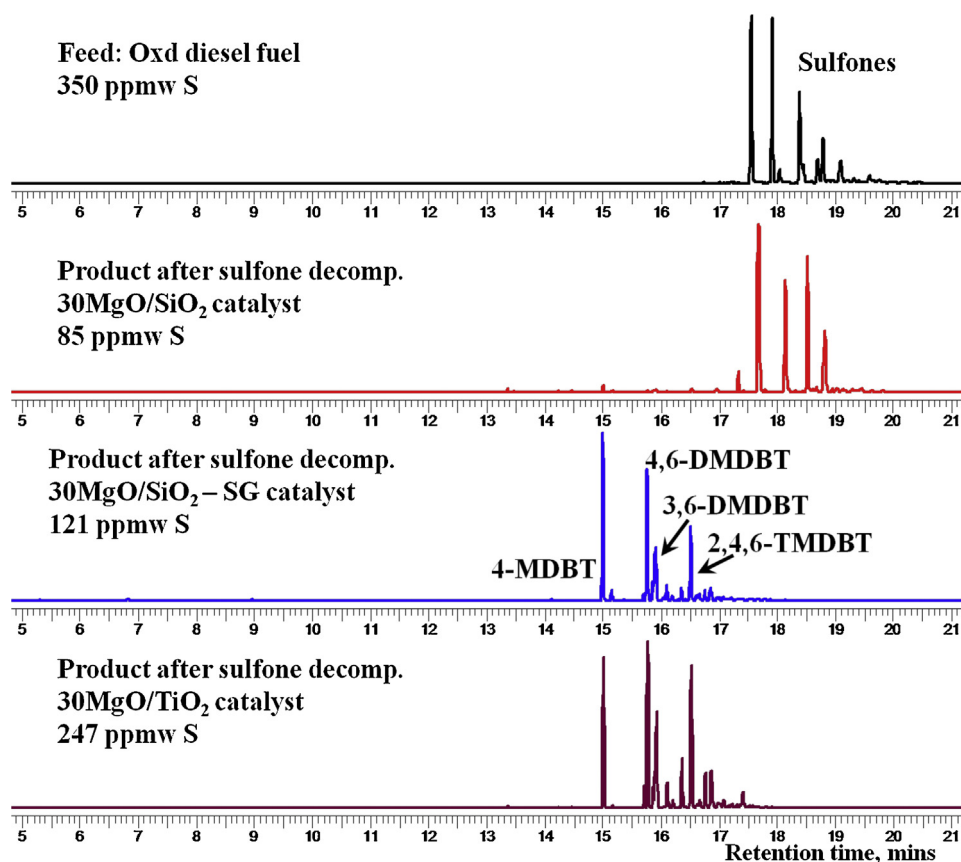


Fig. 3. PFPD chromatographs of pre-oxidized BP-325 diesel fuel containing sulfones and BP-325 diesel fuel after sulfone decomposition on different catalysts (Total S concentrations before and after sulfone decomposition were measured and indicated).

where both acidic and basic catalysts were screened for catalytic cracking of oxidized sulfur compounds in straight run gas oil. Even though beta zeolite [CP 814C from Zeolyst, $\text{SiO}_2/\text{Al}_2\text{O}_3$ mole ratio = 38, surface area = $710 \text{ m}^2/\text{g}$] showed moderate activity for decomposition of oxidized sulfur compounds, significant deoxygenation of oxidized sulfur compounds to parent sulfur compound was observed at 350°C . Although acidic sites might be a plausible cause for undesired conversion of dibenzothiophenic type sulfones to parent sulfur compounds, more detailed effort is required for understanding the effect of SiO_2 synthesis route (including silica source) and its subsequent role in sulfone decomposition.

In comparison to $30\text{MgO}/\text{SiO}_2$ -SG catalyst, $30\text{MgO}/\text{TiO}_2$ showed higher activity for the undesired side reaction. About 71% of the sulfones were converted to sulfur type compounds on this sample which might be due to the nature of TiO_2 based materials which are widely believed to contain oxygen vacancies on the surface [33,34]. It is also interesting to note that even though $30\text{MgO}/\text{TiO}_2$ has higher amount of basic sites than $30\text{MgO}/\text{SiO}_2$ -SG sample (Table 2), it showed poor performance and promoted undesired conversion of dibenzothiophenic type sulfones in the distillate fuel. This indicates that the nature of the support is critical for sulfone decomposition. Since both these catalysts promoted undesired conversion of sulfones back to sulfur compounds, these were not used for further study on sulfone decomposition of real liquid hydrocarbons.

For rest of the catalyst samples, conversion of dibenzothiophenic sulfones to biphenyl type compounds was the only reaction observed. Bulk MgO showed poor activity relative to other samples for conversion of sulfones under the conditions employed in this study. The physical and chemical properties of the supported and bulk MgO are presented in Table 2. Although the number of total basic sites on the commercial bulk MgO-SA is higher than

that on $30\text{MgO}/\text{Al}_2\text{O}_3$ and $30\text{MgO}/\text{SiO}_2$ with comparable surface area, it showed relatively lower activity for sulfone decomposition. Bulk MgO-ME synthesized by direct calcination of magnesium ethoxide had approximately two times more basic site than bulk MgO from Sigma Aldrich and showed higher activity for sulfone decomposition. $30\text{MgO}/\text{SiO}_2$ showed the highest activity for sulfone decomposition (76%) among the samples tested even though the basic sites were three times less in comparison to MgO-ME bulk catalyst. Low loading of MgO on Al_2O_3 gave low activity for sulfone decomposition which might be due to lower number of basic sites on the low loading sample but it performed better than the reference material.

Al_2O_3 and SiO_2 supported samples and bulk MgO were calcined at different temperatures and its effect on the properties of the samples are also shown in Table 2. Increasing calcination temperature resulted in decrease of basic sites and increase in MgO crystallite size. The samples with different MgO crystallite size obtained by calcination at 550°C and 650°C were also tested for sulfone decomposition activity on the same weight basis.

In Fig. 4, the catalyst activity for decomposition of sulfones is plotted versus the MgO crystallite size for the supported and bulk MgO samples calcined at different temperatures. As seen from Fig. 4, there is a good correlation between MgO crystallite size of supported and bulk catalysts and their activity. Going from 40 nm to 180 nm MgO crystallite size the activity for sulfone decomposition decreases from 14.7 to $4.43 \times 10^{-5} \text{ mol S/g/cath}$ as shown in Fig. 4. Even though the basic sites number on MgO-ME bulk catalyst is three times more than that on $30\text{MgO}/\text{SiO}_2$ catalyst, the latter shows better activity for sulfone decomposition. This might be due to the smaller crystallite structure of active sites on the supported SiO_2 sample. The effect of calcination temperature on $30\text{MgO}/\text{Al}_2\text{O}_3$

Table 2
Physical and chemical properties of bulk and supported MgO based catalysts.

Catalyst	Calcination temp (°C)	Surface area (m ² /g)	Pore vol (g/cm ³)	Basic sites ^a (μmol/g)	MgO crystallite size (nm)
MgO-ME	450	252	0.94	1140	84
MgO-SA	450	117	0.22	495	144
30MgO/Al ₂ O ₃	450	126	0.75	359	50
3MgO/Al ₂ O ₃	450	NA	NA	5	-
30MgO/SiO ₂	450	181	1.10	366	43
30MgO/SiO ₂ - SG	450	758	0.98	55	Not detectable
30MgO/TiO ₂	450	28	0.10	359	52
30MgO/Al ₂ O ₃	550	125	0.70	299	75
MgO-ME	650	162	0.72	897	169
30MgO/Al ₂ O ₃	650	128	0.74	218	141
30MgO/SiO ₂	650	175	0.99	52	83

^a - estimated by CO₂-chemisorption (desorption temperature: 50–900 °C).

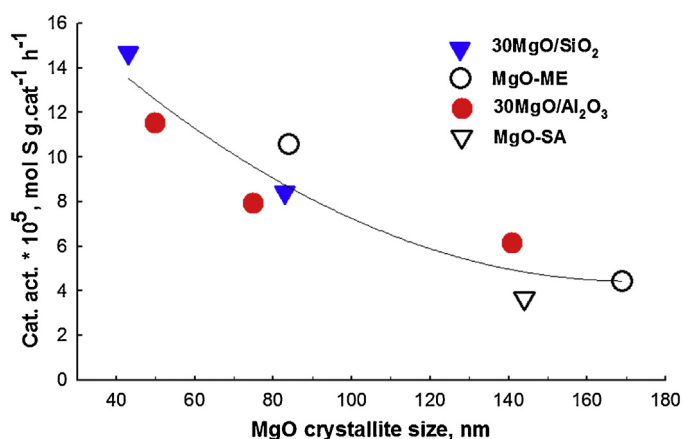


Fig. 4. The influence of MgO crystallite size on catalytic activity for decomposition of oxidized sulfur compounds to sulfur-free hydrocarbons in BP-325 diesel fuel [Reaction conditions: atm pressure; Temp, 450 °C; WHSV, 10 h⁻¹].

is more severe than 30MgO/SiO₂ when the samples were calcined at 650 °C as shown in Table 2 and Fig. 4. It should be noted that although the numbers of basic sites do not appear to correlate directly with sulfone decomposition activity, tailoring materials which have high density of basic sites along with smaller crystallite size of MgO might lead to higher activity sulfone decomposition catalysts.

Fig. 5 shows the effect of MgO crystallite size on turnover frequencies (TOF defined as moles converted per CO₂ uptake site per second) calculated for dibenzothiophenic type sulfone decomposi-

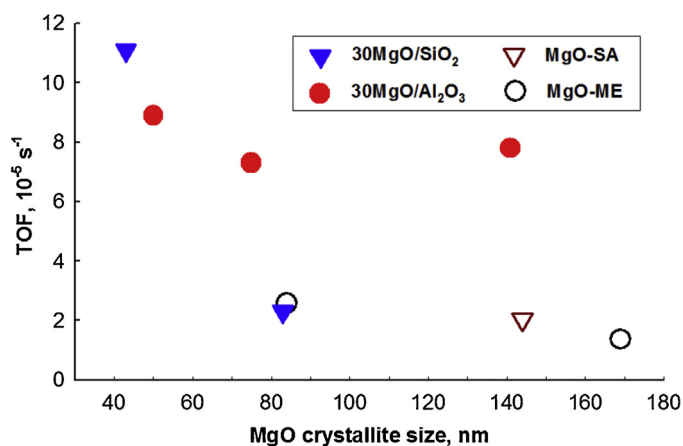


Fig. 5. The influence of MgO crystallite size on TOF [reaction conditions: feed: BP-325 diesel fuel, atm pressure; Temp, 450 °C; WHSV, 10 h⁻¹].

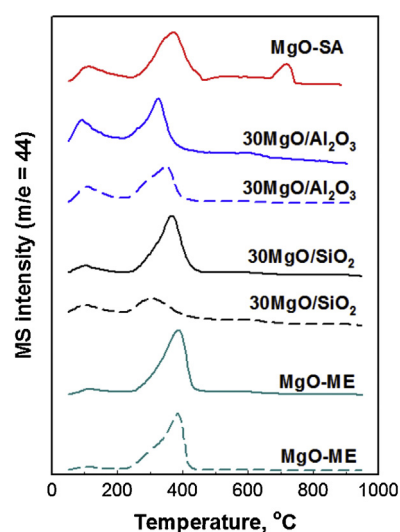


Fig. 6. Distribution of strength of basic sites from CO₂-TPD for selected bulk and supported catalysts [Solid lines: Catalyst calcined at 450 °C. Dash lines: Catalyst calcined at 650 °C].

tion for 30MgO/SiO₂, 30MgO/Al₂O₃, MgO-ME and MgO-SA samples. MgO crystallite sizes of <60 nm are obtained on SiO₂ and Al₂O₃-supported catalysts as evident from Fig. 5. Correspondingly the highest TOF are obtained on these samples. It is interesting to note that TOF is independent of MgO crystallite size in the case of 30MgO/Al₂O₃ catalyst. This shows that the nature of active sites remain similar even with increasing crystallite size or calcination temperature on Al₂O₃-supported MgO catalyst. Similar observation was found on the unsupported MgO-ME catalyst even though the specific-surface activity of MgO-ME catalyst is about 3.5 to 4 less than that of 30MgO/Al₂O₃ catalyst. Increasing MgO crystallite size on 30MgO/SiO₂ has detrimental effect on TOF as shown by five times decrease in catalytic activity in Fig. 5. This shows that the nature of active sites change with increasing crystallite size of MgO when supported on SiO₂. The catalyst samples were calcined at 450 °C and 650 °C and the corresponding crystallite sizes of MgO are also presented in Table 2. There appears to be no direct correlation between catalyst activity and the total amount of basic sites.

Fig. 6 presents the relative distribution of the strength of basic sites obtained by CO₂-TPD on the MgO-ME, 30MgO/Al₂O₃ and 30MgO/SiO₂ catalysts. All catalysts show a dominant peak centered between 300 and 400 °C indicating that relative basic strength distribution of the unsupported and unsupported MgO catalysts might be the same under the CO₂-TPD conditions tested. 30MgO/Al₂O₃ and 30MgO/SiO₂ show similar CO₂ desorption peaks when calcined at 450 °C. In addition to the peak between 300 and 400 °C,

both catalysts exhibit weak CO₂ desorption peak at 100 °C. This is consistent with earlier studies on MgO supported catalysts. Different CO₂ desorption behaviors were observed for 30MgO/Al₂O₃ and 30MgO/SiO₂ catalysts when calcined at 650 °C. The peak observed between 300 and 400 °C was still dominant when 30MgO/Al₂O₃ catalyst is calcined at 650 °C. Relative to the sample calcined at 450 °C, the peak is shifted a little which might be due to probable MgAl₂O₄ type spinel formation when calcined at higher temperatures. Studies in the past have revealed that MgAl₂O₄ formation is not significant at calcination temperatures of 450 °C but become dominant at higher temperature forming this stable oxide phase [35]. This is consistent with the earlier observation where TOF independent of MgO crystallite size was seen on 30MgO/Al₂O₃ sample. It should be noted that although the basic strength distribution of 30MgO/Al₂O₃ catalyst remains the same even when calcined at 650 °C, there is a significant drop in activity which might be related to the increased agglomeration of MgO as evident by the crystallite size of MgO presented in Fig. 4.

In contrast to 30MgO/Al₂O₃ sample, there was a significant decrease in the CO₂ desorption peak observed between 300 and 400 °C for the 30MgO/SiO₂ sample when calcined at 650 °C. The total basic site number estimated by CO₂-TPD decreases from 366 μmol/g to 52 μmol/g when calcined at 650 °C. This shows that potential adverse interaction occurs when 30MgO/SiO₂ is calcined at higher temperatures resulting in agglomeration and neutralization of the basic sites. More detailed study is required to understand the role of SiO₂ for MgO based catalysts for sulfone decomposition reactions. The low temperature CO₂ desorption peak was observed on both the supported catalysts at calcination temperatures of 450 °C and 650 °C. Even with the presence of weak CO₂ desorption peak for the 30MgO/SiO₂ sample calcined at 650 °C, there was a significant drop in activity when the catalyst was calcined at 650 °C indicating that relatively stronger basic site represented by peak centered between 300 and 400 °C might be more critical for sulfone decomposition reactions.

Unsupported MgO-ME and MgO-SA catalysts showed desorption band between 300 and 400 °C indicative of bulk MgO species. A low temperature desorption peak was observed at 120 °C for MgO-SA catalyst but was not prominent on MgO-ME catalyst. Analysis of MgO-SA by CO₂-FTIR which is discussed later indicated the presence of hydroxyl groups on MgO-SA catalyst. The low temperature CO₂ desorption peak might be indicative of bicarbonate type species on MgO-SA sample. It should be noted that low temperature peak observed on bulk MgO-SA and the supported samples are of different nature [36–38]. In contrast to other samples, low temperature CO₂ desorption peak was not prominent on MgO-ME sample. Also MgO-SA sample obtained from Sigma Aldrich was ≥99% pure and was used after calcination at 450 °C under air. A high temperature CO₂ desorption peak was observed around 720 °C for MgO-SA sample might be due to the presence of ≤1% of other trace elements in the sample used in this study.

It should be noted that although this study shows the potential effect of MgO crystallite size and the nature of support on activity and selectivity of sulfones decomposition, a further detailed study is warranted for understanding the causes for activity and selectivity differences. As presented in Fig. 4, early analyses of this study shows that particle size can be a key determining factor for sulfone decomposition activity but it is also plausible that specific facets of MgO might be formed or remains stable with change in crystallite size of MgO. For example, a recent structure-sensitivity study by Montero et al. [39] on MgO based materials showed that different basic surfaces are exposed by varying calcination temperatures. They reported that low temperature calcination exposed weakly basic (100) surfaces with high temperature resulting in the formation of basic (110) and (111) surfaces [39]. Understanding of surface electronic structures of MgO based materials and

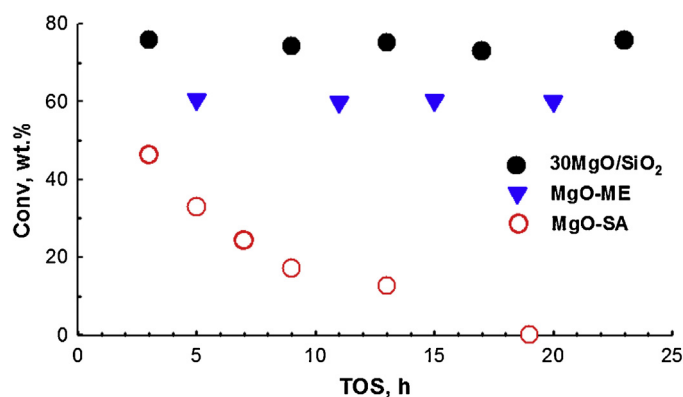


Fig. 7. Time on stream profiles for catalytic decomposition of oxidized sulfur compounds in BP-325 diesel fuel over MgO based catalysts [Initial S, 325 ppmw; temperature, 450 °C; WHSV, 10 h⁻¹].

correlating them with activity for sulfone decomposition might lead to a better understanding of structure-activity/selectivity relationship.

3.2. Time on stream activity tests

Since 30 MgO/SiO₂ gave the highest activity for sulfone decomposition, it was further examined for time on stream activity and was compared with bulk MgO-ME. Reference sample, MgO-SA was also tested for time on stream activity. All catalysts were calcined at 450 °C before testing.

Fig. 7 presents the time on stream profiles for catalytic decomposition of oxidized sulfur compounds in diesel fuel. Time on stream data obtained in this study provides a comparison between MgO-ME, MgO-SA and 30MgO/SiO₂ catalysts to gain an understanding on factors that affect catalyst stability. As seen from Fig. 7, MgO-SA completely deactivates after 19 h on stream whereas 30MgO/SiO₂ catalyst demonstrates good steady state activity for as long as 23 h. Also, bulk MgO-ME showed steady state activity in contrast to MgO-SA sample. As discussed earlier MgO-SA used in this study is ≥99% pure, although some deactivation might be caused by the presence of ≤1% of other trace elements, no steady state activity even after a period of deactivation was observed on MgO-SA catalyst as shown in Fig. 7. This indicates the nature of active sites on the surface of MgO-SA might be different from the bulk and supported catalysts derived from magnesium ethoxide precursor potentially causing deactivation of MgO-SA catalyst with time. Also, 30MgO/SiO₂-SG and 30MgO/TiO₂ catalysts which showed undesired selectivity for dibenzothiophene sulfone decomposition as presented in Fig. 2 did not show any change in product selectivity during 6 h time on stream runs but they were not tested further for longer hours. It should be noted that the data presented in Fig. 7 is not sufficient to evaluate catalyst life and stability.

Fig. 8 presents the time on stream data for decomposition of oxidized sulfur compounds in jet fuel. In contrast to dibenzothiophene type sulfone decomposition, 30MgO/SiO₂ was more active for decomposition of benzothiophenic type sulfones found in jet fuel even at 400 °C. The 30MgO/SiO₂ catalyst shows higher activity for decomposition of benzothiophenic sulfones than dibenzothiophenic type sulfone as seen from Figs. 7 and 8. Benzothiophenic type sulfone decomposition based on MgO-SA showed deactivation profile similar to dibenzothiophene type sulfone decomposition as seen from Figs. 7 and 8.

Given the difference in activity and stability of 30MgO/SiO₂, MgO-ME and MgO-SA catalysts, they were analyzed by infrared spectroscopy to understand the nature of basic sites on these samples. CO₂-FTIR spectra of the fresh catalysts evaluated for time on

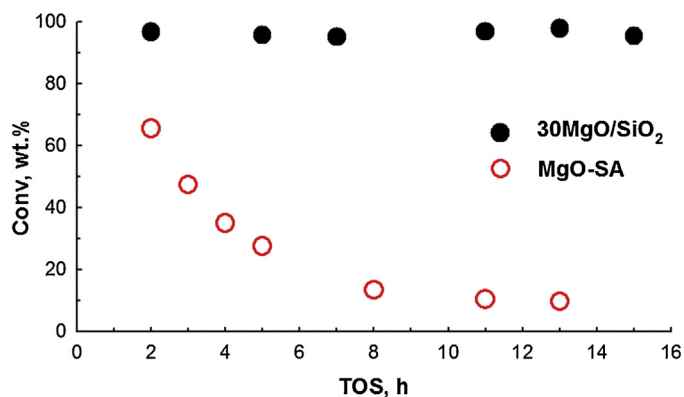


Fig. 8. Time on stream profiles for catalytic decomposition of oxidized sulfur compounds in JP-5 jet fuel (Initial S, 1050 ppmw; temperature, 400 °C; WHSV, 10 h⁻¹).

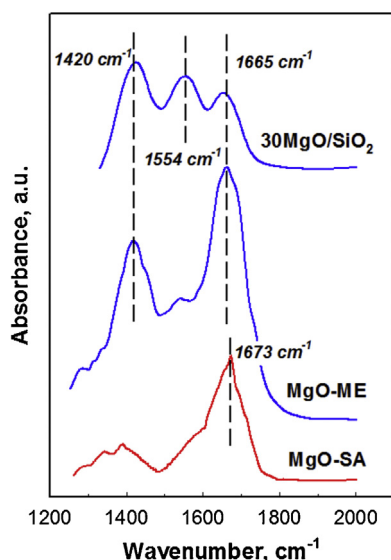


Fig. 9. CO₂-FTIR analysis of 30MgO/SiO₂, MgO-ME and MgO-SA fresh catalysts.

stream activity tests are presented in Fig. 9. A qualitative analysis indicates that the spectra are complex and different types of basic sites are present on the supported and bulk catalysts. For the supported 30MgO/SiO₂ catalyst, three strong vibration bands are observed at approximately 1420 cm⁻¹, 1554 cm⁻¹, and 1665 cm⁻¹ representing non-coordinated, monodentate and bidentate carbonates, respectively [40,41]. In contrast to supported 30MgO/SiO₂ catalyst, bulk MgO-ME catalyst was not characterized by the presence of strong vibration band of monodentate carbonates at 1554 cm⁻¹. MgO in 30MgO/SiO₂ and MgO-ME were derived from the same magnesium ethoxide precursor. In contrast to 30MgO/SiO₂ and MgO-ME, the commercial MgO-SA did not show strong vibration bands of 1420 and 1554 cm⁻¹. Bidentate carbonate species formed through coordination of CO₂ with Mg²⁺-O²⁻ acid-base pair sites were detected at 1665 cm⁻¹ for 30MgO/SiO₂ and MgO-ME catalyst. But for commercial bulk MgO-SA catalyst, there was a shift in the peak to 1673 cm⁻¹. Similar studies on analysis of MgO with different surface properties by CO₂-FTIR have revealed that overlapped absorption from hydrogen carbonates (hydroxyl groups on the surface) should be considered in the bidentate absorption region. An 8 cm⁻¹ shift was observed between CO₂ adsorption on hydroxyl group and O²⁻ centers representing hydrogen carbonate and bidentate carbonate species by several authors [41,42]. In this study, the bands observed at 1665 cm⁻¹ for 30MgO/SiO₂ and MgO-ME catalyst was shifted to 1673 cm⁻¹ for

Table 3

Mg 2p and O 1s features of fresh and spent MgO based catalysts.

Catalyst	30MgO/SiO ₂		MgO-SA	
	Mg 2p	O 1s	Mg 2p	O 1s
Fresh	50.2	531.6	49.2	531.7
Spent	50.5	532.0	49.7	532.3

Catalytic reaction for spent catalyst: BP-325 diesel fuel (initial S concentration, 325 ppmw; temperature, 450 °C; WHSV, 10 h⁻¹).

the bulk MgO-SA catalyst which potentially represents a hydrogen carbonate vibration band. O 1s feature obtained by XPS analysis of MgO-SA bulk catalyst revealed two distinct features (data not shown here) which was not identified on the 30MgO/SiO₂ and bulk MgO-ME catalyst indicating the possibility of hydroxyl groups on the surface of MgO-SA. This difference in the nature of basic site on MgO-SA catalyst might explain the deactivation of the catalyst when it was tested for sulfone decomposition in JP-5-1050 jet and BP-325 diesel fuels which is in contrast to 30MgO/SiO₂ and MgO-ME catalysts. CO₂-FTIR spectra presented here show that TOF based on total CO₂ uptake (Fig. 5) is a qualitative measurement as different types of basic sites are observed on the supported and unsupported catalysts. More in-depth study and quantification of TOF based on specific type of basic sites by CO₂-FTIR are warranted to better understand structure/activity relationship.

Further, fresh and spent 30MgO/SiO₂ and MgO-SA catalyst obtained from decomposition of sulfones in JP-5-1050 jet and BP-325 diesel fuels were analyzed by DRIFTS (FTIR) and the results are shown in Fig. 10. Spectra (3) and (4) represent fresh and spent MgO-SA catalysts, respectively. As seen from Fig. 10a and 10b, a peak centered at 1250 cm⁻¹ representing sulfonic group was present on the spent MgO-SA catalyst (marked as * on spent MgO-SA spectra) [43,44]. We believe this sulfonic group is part of -SO₃H species that is formed on the surface of the MgO-SA catalyst containing hydroxyl groups potentially through an organic intermediate after homolytic scission of one of -C-SO₂ bond in benzothiophene or dibenzothiophene type sulfone. This might be the cause for deactivation of the catalyst. In the absence of hydroxyl groups on the surface like in the case of 30MgO/SiO₂ and MgO-ME catalyst, the intermediate after the homolytic scission of one of the -C-SO₂ bond would be -SO₃²⁻ because of O²⁻ nature of basic sites. Further homolytic scission would result in the formation of sulfur-free hydrocarbon product with SO₂ liberated from the surface of the catalyst.

Fresh and spent 30MgO/SiO₂ samples were analyzed before and after time on stream and no sulfur based vibrations were found on the sample as shown by spectra (1) and (2) in Fig. 10a and b. The broad peak centered around 1200 cm⁻¹ represents the Si content of 30MgO/SiO₂ catalyst [45].

In an effort to confirm that significant SO₂ adsorption does not occur during the decomposition reaction, fresh catalyst (30MgO/SiO₂ and MgO-SA) and the corresponding spent catalysts obtained after decomposition of sulfones in BP-325 diesel fuel were analyzed by XPS. Positions of Mg 2p and O 1s features of the catalysts are tabulated in Table 3. As seen from the data, there was no significant shift in the peak positions of Mg 2p and O 1s features. In the region between 160 and 178 eV for S 2p feature, there was no sulfate or sulfite peaks visible on the spent catalysts (S 2p not shown) indicating that there is no significant MgSO₃ or MgSO₄ formation via SO₂ chemisorption under the reaction conditions employed in this study. There is also a detection limit especially for sulfur in low concentration by XPS which has been confirmed by a recent study in which a catalyst containing 0.3 wt% sulfur did not show any S 2p feature [46]. Also the detection limit in XPS depends upon the atom, the nature of the sample and instrumental parameters but a typical value is 0.1 at% [47,48]. This shows that

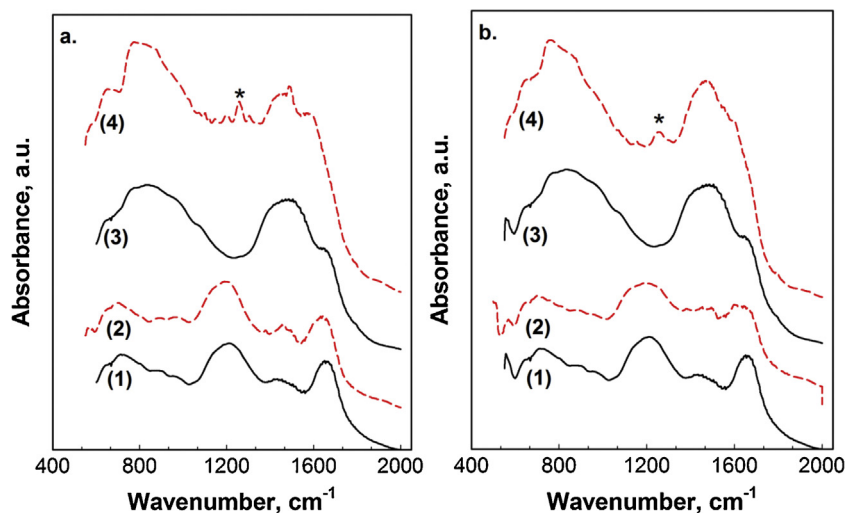


Fig. 10. FTIR analysis of fresh and spent catalysts [(1) fresh 30MgO/SiO₂, (2) spent 30MgO/SiO₂, (3) fresh MgO-SA, (4) spent MgO-SA] after catalytic decomposition of oxidized sulfur compounds (a) JP-5-1050 jet fuel (Initial S, 1050 ppmw; temperature, 400 °C; WHSV, 10 h⁻¹) (b) BP-325 diesel fuel (Initial S, 325 ppmw; temperature, 450 °C; WHSV, 10 h⁻¹) [* surface -SO₃H species [50]].

SO₂ adsorption is not dominant pathway of this decomposition reaction.

3.3. Effect of reaction temperature on sulfone decomposition by 30MgO/SiO₂ catalyst

The effect of temperature on activity for decomposition of oxidized sulfur compounds in both jet and diesel fuels was studied over 30MgO/SiO₂ and the time on stream profiles are presented in Figs. 11 and 12. From the data presented in Figs. 11 and 12, it can be inferred that the supported MgO based materials are more active for decomposition of benzothiophenic sulfones than dibenzothiophenic type sulfones. Decomposition of oxidized sulfur compounds in BP-325 diesel at 400 °C results in rapid deactivation of the catalyst in 10 h. In contrast, steady state activity was observed for decomposition of sulfones in JP-5-1050 jet fuel at 400 °C. But reducing the decomposition temperature from 400 to 320 °C resulted in deactivation of the 30MgO/SiO₂ catalyst for JP-5-1050 jet fuel. The cause of deactivation of the catalyst might be due to reduced activity for homolytic scission of C-SO₂ bonds in sulfones and shows that lower temperatures are not favorable for decomposition reaction. FTIR (DRIFTS) analysis of spent 30MgO/SiO₂ catalyst tested at lower temperature did not show any distinct sulfur based vibration on the surface.

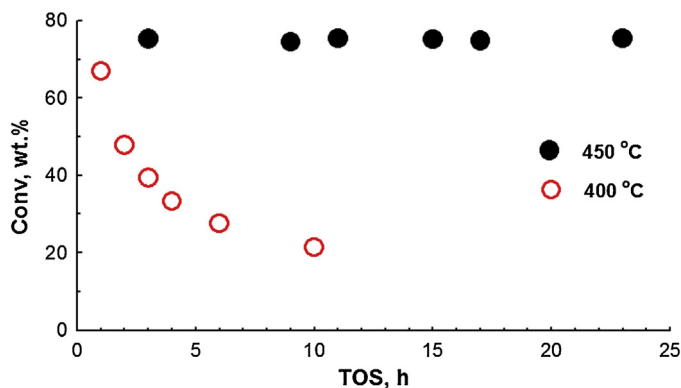


Fig. 11. Effect of reaction temperature on decomposition of oxidized sulfur compounds in BP-325 diesel fuel over 30MgO/SiO₂ catalyst [Initial S, 325 ppmw; WHSV, 10 h⁻¹].

3.4. Model sulfone decomposition over MgO based materials

To understand the nature of the products obtained from decomposition of sulfones, surrogate hydrocarbon liquid feeds containing 3-methyl benzothiophene sulfone and dibenzothiophene sulfone were studied. Unlike organic sulfur compounds, oxidized sulfur compounds have very low solubility in paraffinic solvents. So to ensure complete solubility of sulfones, aromatic rich hydrocarbons including alkyl benzene and tetrahydronaphthalene were preferred solvents. In an effort to eliminate overlap of sulfones and the products from decomposition of sulfones with the solvents used in the preparation of model feedstock, different mix of aromatic rich solvents were used for 3-methyl benzothiophene sulfone and dibenzothiophene sulfone, as shown in Table 1.

Catalytic activity of surrogate hydrocarbon feeds tested in this study were recorded at specific TOS (time on stream) of 4 h for all runs. Products obtained from catalytic and non-catalytic decomposition of sulfones in model feeds is presented as Table 4. As oxidized sulfur compounds in JP-5 jet fuel was active at 400 °C, 3-methyl benzothiophene sulfone decomposition was studied at 400 °C over 30MgO/SiO₂-SG catalyst prepared by sol-gel method. The major product obtained from 3-methyl benzothiophene sulfone decomposition was iso-propyl benzene. Undesired conversion of 3-methyl benzothiophene sulfone through oxygen removal to

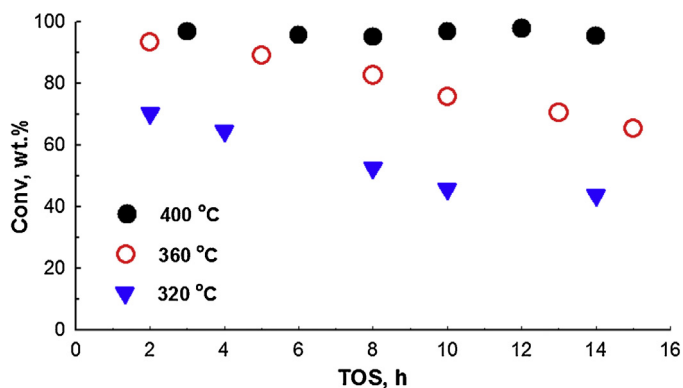


Fig. 12. Effect of reaction temperature on decomposition of oxidized sulfur compounds in JP-5-1050 jet fuel over 30MgO/SiO₂ catalyst [Initial S, 1050 ppmw; WHSV, 10 h⁻¹].

Table 4
Product distribution from catalytic and non-catalytic decomposition of sulfones in model feedstock.

No	S compound	Catalyst	T, (°C)	Conv., (%)	Products	Yield, mol (%)	Note
1.	3-methyl BTO ₂	30MgO/SiO ₂ -SG	400 [*]	100	Iso-propyl benzene Benzothiophene 4-hydroxybenzenesulfonic acid	76.4 13.9 9.4	This Study
2.	DBTO ₂	30MgO/SiO ₂ -SG	450 [*]	100	Biphenyl Dibenzothiophene	76.1 23.3	
3.	DBTO ₂	30MgO/SiO ₂	450 [*]	90	Biphenyl	89.8	
4.	DBTO ₂	Glass beads	450 [*]	13.9	Biphenyl Dibenzothiophene	8.9 4.6	
5.	DBTO ₂	Na ₂ O ^{**}	300	70.0	Biphenyl	69.7	
6.	BTO ₂	NaOH	300 [#]	100	Sodium-2-methyl benzene sulfonate Sodium-2-methyl phenolate Sodium sulfite Sodium carbonate Benzene Dibenzofuran Biphenyl	>50 27.4 31.6 6.4 >90.0 ~5	
7.	DBTO ₂	NaOH	300 [#]	100			Ref [27]

^{*} Fixed bed reactor; contact time, WHSV, 10 h⁻¹ (catalytic and non-catalytic activity were recorded at specific TOS (time on stream) of 4 h for all runs).

^{**} Batch reactor, Na₂O/sulfone (molar ratio)—3; reaction time, 4 h.

[#] Batch reactor; NaOH/sulfone (molar ratio)—5; reaction time, 4 h.

benzothiophene was observed on 30MgO/SiO₂-SG. Formation of benzothiophene as an undesired product also shows that dealkylation is also one of the reaction pathways under the conditions tested in the study. Dibenzothiophene sulfone decomposition was studied at 450 °C over 30MgO/SiO₂ and biphenyl was observed as the major product. Consistent with the results obtained from decomposition of dibenzothiophenic type sulfones in BP-325 diesel fuel, there was undesired conversion of dibenzothiophene sulfone model compound to dibenzothiophene over 30MgO/SiO₂-SG catalyst at 450 °C. A non-catalytic run in presence of glass beads at 450 °C gave low conversion of dibenzothiophene sulfone. The distribution of products from decomposition of benzothiophene and dibenzothiophene type sulfones demonstrates the effectiveness of MgO based materials.

In addition to products obtained from decomposition of sulfones in model feeds, products obtained from decomposition of model sulfones from a previous study using NaOH are also included in Table 4. Products obtained from decomposition of model sulfones from a previous study are also included in Table 4. As seen from the product distribution, completely different products were obtained by NaOH based decomposition of sulfones. Sodium salts of organic compounds were obtained by decomposition of benzothiophene sulfone over NaOH. Dibenzothiophene sulfone decomposition over NaOH gave dibenzofuran as the major product and small amounts of biphenyl which is in contrast to our study. In a previous study [40,41], a multistep reaction pathway was proposed for decomposition of dibenzothiophene sulfone over molten NaOH at 300 °C with a NaOH/dibenzothiophene sulfone molar ratio of 5. Wallace and Heimlich observed sodium-2-phenyl phenolate as the major product but with extended residence time dibenzofuran was formed as the major product [40,41]. Although this results in dibenzothiophene sulfone decomposition to a sulfur-free hydrocarbon, addition of oxygen necessitates further downstream processing to obtain oxygen free hydrocarbon product. Under similar conditions, they observed rapid conversion of benzothiophene sulfone but with sodium-2-methyl benzene sulfonate and sodium-2-methyl phenolate as major products [40,41].

To understand the difference in product distribution between an oxide and hydroxide, we further tested the decomposition of dibenzothiophene sulfone over Na₂O under conditions similar to the above study carried out by Wallace and Heimlich. Interestingly, biphenyl was observed as the major product over Na₂O, which is in contrast to NaOH based decomposition where dibenzofuran was obtained as the major product. This clearly demonstrates that

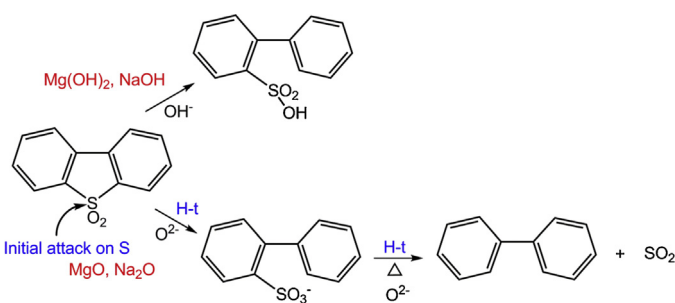


Fig. 13. Plausible reaction pathway and possible intermediates for catalytic decomposition of dibenzothiophene sulfone over MgO and Na₂O based catalysts containing hydroxide ion and oxide ion type species as basic sites (temperature, 450 °C; initial S, 350 ppmw; WHSV, 10 h⁻¹).

different sulfone decomposition pathways take place on an oxide and hydroxide of sodium.

Based on product distribution of dibenzothiophene sulfone decomposition over 30MgO/SiO₂, Na₂O and NaOH, and deactivation observed on MgO-SA catalyst for decomposition of sulfones in BP-325 diesel fuel, a plausible reaction pathway is shown in Fig. 13. The initial step in the decomposition of sulfone over alkali/alkaline metal oxide appears to be a catalytic homolytic scission of C–SO₂ bond with rapid radical capping by internal hydrogen transfer (H-t) from other components in the feed to produce a sulfonate type organic intermediate species on the surface. Hydrogen transfer from hydrocarbons to radicals are well known to be feasible under the conditions employed. Under the decomposition conditions employed, further homolytic scission of –C–SO₃– group (potential surface intermediate) results in expulsion of the sulfur-free aromatic ring. This pathway leads to the formation of biphenyl as the major product from dibenzothiophene sulfone decomposition of alkali/alkaline metal oxide. Similar sulfonate type intermediate was proposed by Wallace and Heimlich when they observed very low yields of biphenyl from dibenzothiophene sulfone decomposition over NaOH [40,41]. But the major product obtained from their study was dibenzofuran as shown in Table 4. The SO₂ on the surface is expelled because the equilibrium for MgSO₃ decomposition is favored under the thermal conditions employed in this study. This was confirmed by obtaining bulk thermodynamic calculations of MgSO₃ decomposition with HSC chemistry software (v.5.1). Also an earlier study showed that at temperatures above 350 °C, all of the SO₂ are completely removed from the surface of

MgO [49]. In contrast, on MgO based material containing hydroxide species probably results in the formation of $-SO_3H$ type organic intermediate on the surface by homolytic scission of one of the $-C-SO_2$ bond. The formation of sulfonic acid organic surface intermediate can potentially form resonance with aromatic compound resulting in stable intermediate. As discussed earlier, the formation of this $-SO_3H$ type intermediate was confirmed by DRIFTS (FTIR) when the spent MgO-SA catalyst was tested for sulfone decomposition of JP-5-1050 jet and BP-325 diesel fuels as shown in Fig. 10a and 10b. More detailed discussion of these reactions is unjustified based on the present data, but model compound work carried out in this study clearly demonstrates preferred product distribution over catalysts tested in this study with formation of biphenyl and iso-propyl benzene from dibenzothiophene sulfone and 3-methyl benzothiophene sulfone, respectively.

4. Conclusions

A series of bulk and supported MgO based catalysts was prepared and tested for decomposition of sulfones in real liquid hydrocarbon fuels. Among the catalysts tested, 30MgO/SiO₂ prepared by wet impregnation procedure showed the best activity for decomposition of sulfones in jet and diesel fuel fuels, averaging 97 and 76%, respectively. The type of support and the nature of sites play a critical role in sulfone decomposition chemistry as evident by undesired conversion of dibenzothiophenic sulfones back to parent sulfur compound over 30MgO/TiO₂ (prepared by wet impregnation) and 30MgO/SiO₂-SG (prepared by sol-gel) catalysts. This shows that potential nature of active sites (oxygen vacancies in the case of TiO₂-supported catalyst and acidic sites in the case of 30MgO/SiO₂-SG catalyst) might play an important role in determining the selectivity of dibenzothiophenic sulfone decomposition. Analysis suggests that higher activity for sulfone decomposition is associated with smaller MgO crystallite size and not necessarily by higher basicity of the catalyst measured by CO₂-chemisorption. In terms of surface-specific activity, supported 30MgO/SiO₂ catalyst was four times more active than bulk MgO-ME catalyst prepared by thermal decomposition of magnesium ethoxide. Consistent steady state activity was observed from time on stream testing of 30MgO/SiO₂ and bulk MgO-ME catalysts for decomposition of dibenzothiophenic type sulfones at 450 °C. Under similar conditions, significant deactivation was observed on the commercial bulk MgO-SA catalyst. CO₂-FTIR analysis of the fresh catalyst revealed that the types of basic sites on MgO-SA catalyst were different from those present on 30MgO/SiO₂ and MgO-ME catalysts. Also, analysis of the deactivated MgO-SA catalyst by FTIR (DRIFTS) revealed the presence of sulfonic vibrations potentially causing the catalyst to deactivate. Model compounds decomposition of 3-methyl benzothiophene sulfone and dibenzothiophene sulfone over the supported MgO based materials gave iso-propyl benzene and biphenyl as the major products probably through a homolytic scission of the $-C-SO_2$ bonds found in sulfone type of compounds.

Acknowledgements

The authors gratefully acknowledge the support for our desulfurization research in part by the U.S. Office of Naval Research and NAVSEA Philadelphia through a grant, and by the U.S. Army Research Laboratory through a SBIR grant sub-contract with Altex Technologies. Discussions with Dr. Naoto Koizumi of Pennsylvania State University were very helpful. Assistance from staff at Materials Research Institute for catalyst characterization and from EMS Energy Institute for chemical orders is acknowledged. The authors thank Dr. Xiaochun Xu and Dr. Manuel Francisco of Exxon Mobil Research and Engineering for kindly reviewing the manuscript. The

authors also wish to acknowledge the two anonymous reviewers for providing helpful comments.

References

- [1] C. Song, *Catalysis Today* 86 (2003) 211–263.
- [2] E. Ito, J.A.R. van Veen, *Catalysis Today* 116 (2006) 446–460.
- [3] A. Stanislaus, A. Marafi, M.S. Rana, *Catalysis Today* 153 (2010) 1–68.
- [4] A. Ishihara, D. Wang, F. Dumeignil, H. Amano, E.W. Qian, T. Kabe, *Applied Catalysis A: General* 279 (2005) 279–287.
- [5] J. Zhang, A. Wang, X. Li, X. Ma, *Journal of Catalysis* 279 (2011) 269–275.
- [6] D. Wang, E.W. Qian, H. Amano, K. Okata, A. Ishihara, T. Kabe, *Applied Catalysis A: General* 253 (2003) 91–99.
- [7] R. Sundararaman, X. Ma, C. Song, *Industrial and Engineering Chemistry Research* 49 (2010) 5561–5568.
- [8] S. Murata, K. Murata, K. Kidena, M. Nomura, *Energy and Fuels* 18 (2003) 116–121.
- [9] X. Ma, A. Zhou, C. Song, *Catalysis Today* 123 (2007) 276–284.
- [10] US Patent Publication No. US2003/6596914 B2, Method of desulfurization and dearomatization of petroleum liquids by oxidation and solvent extraction, 2003.
- [11] B.N. Heimlich, T.J. Wallace, *Tetrahedron* 22 (1966) 3571–3579.
- [12] A. Chica, A. Corma, M.E. Dómine, *Journal of Catalysis* 242 (2006) 299–308.
- [13] J. Chang, A. Wang, J. Liu, X. Li, Y. Hu, *Catalysis Today* 149 (2010) 122–126.
- [14] J.T. Sampanthar, H. Xiao, J. Dou, T.Y. Nah, X. Rong, W.P. Kwan, *Applied Catalysis B: Environmental* 63 (2006) 85–93.
- [15] R. Sundararaman, X.L. Ma, C.S. Song, *Industrial and Engineering Chemistry Research* 49 (2010) 5561–5568.
- [16] A. Di Giuseppe, M. Crucianelli, F. De Angelis, C. Crestini, R. Saladino, *Applied Catalysis B: Environmental* 89 (2009) 239–245.
- [17] S. Otsuki, T. Nonaka, W. Qian, A. Ishihara, T. Kabe, *Journal of the Japan Petroleum Institute* 42 (1999) 315–320.
- [18] M.R. Khan, E. Al-Sayed, *Energy Sources Part a—Recovery Utilization and Environmental Effects* 30 (2008) 200–217.
- [19] US Patent Publication No. US2001/6277271 B1, Process for the desulfurization of a hydrocarbonaceous oil, 2001.
- [20] N. You, M.J. Kim, K.E. Jeong, S.Y. Jeong, Y.K. Park, J.K. Jeon, *Journal of Nanoscience and Nanotechnology* 10 (2010) 3663–3666.
- [21] R. Sundararaman, Catalytic oxidative desulfurization of liquid hydrocarbon feedstocks using air, The Pennsylvania State University, University Park, PA, 2011.
- [22] H. Kim, K.-E. Jeong, S.-Y. Jeong, Y.-K. Park, D.H. Kim, J.-K. Jeon, *Journal of Nanoscience and Nanotechnology* 11 (2011) 1706–1709.
- [23] M.J. Kim, H. Kim, K.-E. Jeong, S.-Y. Jeong, Y.K. Park, J.-K. Jeon, *Journal of Industrial and Engineering Chemistry* 16 (2010) 539–545.
- [24] Y.K. Park, S.Y. Kim, H.J. Kim, K.Y. Jung, K.-E. Jeong, S.-Y. Jeong, J.-K. Jeon, *Korean Journal of Chemical Engineering* 27 (2010) 459–464.
- [25] S. Otsuki, T. Nonaka, N. Takashima, W. Qian, A. Ishihara, T. Imai, T. Kabe, *Energy and Fuels* 14 (2000) 1232–1239.
- [26] US Patent Publication No. US2002/6368495 B1, Removal of sulfur-containing compounds from liquid hydrocarbon streams, 2002.
- [27] T.J. Wallace, B.N. Heimlich, *Tetrahedron* 24 (1968) 1311–1322.
- [28] T. Aida, T.G. Squares, C.G. Venier, *Tetrahedron Letters* 24 (1983) 3543–3546.
- [29] R.B. LaCount, S. Friedman, *The Journal of Organic Chemistry* 42 (1977) 2751–2754.
- [30] European Patent No. EP2496538 A1, Hydrocarbon recovery from sulfones formed by oxidative desulfurization process, 2012.
- [31] US Patent Publication No. US2013/0030236 A1, Process for oxidative desulfurization with integrated sulfone decomposition, 2013.
- [32] M. Balíková, L. Beránek, *Collection of Czechoslovak Chemical Communications* 40 (1975) 3108–3113.
- [33] I. Nakamura, N. Negishi, S. Kutsuna, T. Ihara, S. Sugihara, K. Takeuchi, *Journal of Molecular Catalysis A: Chemical* 161 (2000) 205–212.
- [34] S. Wendt, R. Schaub, J. Matthiesen, E.K. Vestergaard, E. Wahlström, M.D. Rasmussen, P. Thøstrup, L.M. Molina, E. Lægsgaard, I. Stensgaard, B. Hammer, F. Besenbacher, *Surface Science* 598 (2005) 226–245.
- [35] D.-E. Jiang, B. Zhao, Y. Xie, G. Pan, G. Ran, E. Min, *Applied Catalysis A: General* 219 (2001) 69–78.
- [36] X. Fu, *Advanced Materials Research* 476 (2012) 1811–1814.
- [37] L. Li, X. Wen, X. Fu, F. Wang, N. Zhao, F. Xiao, W. Wei, Y. Sun, *Energy & Fuels* 24 (2010) 5773–5780.
- [38] J. Di Cosimo, V. Diez, M. Xu, E. Iglesia, C. Apesteguía, *Journal of Catalysis* 178 (1998) 499–510.
- [39] J.M. Montero, P. Gai, K. Wilson, A.F. Lee, *Green Chemistry* 11 (2009) 265–268.
- [40] M.B. Cerfontain, J.A. Moulijn, *Fuel* 65 (1986) 1349–1355.
- [41] A.O. Menezes, P.S. Silva, E.P. Hernandez, L.E.P. Borges, M.A. Fraga, *Langmuir* 26 (2010) 3382–3387.
- [42] R. Philipp, K. Fujimoto, *The Journal of Physical Chemistry* 96 (1992) 9035–9038.

- [43] Y. Woo, S.Y. Oh, Y.S. Kang, B. Jung, *Journal of Membrane Science* 220 (2003) 31–45.
- [44] M. Balbasi, B. Gözütok, *Synthetic Metals* 160 (2010) 150–155.
- [45] R.F.S. Lenza, W.L. Vasconcelos, *Materials Research* 4 (2001) 175–179.
- [46] C. Xie, Y. Chen, Y. Li, X. Wang, C. Song, *Applied Catalysis A: General* 390 (2010) 210–218.
- [47] R.I. Hegde, P.J. Tobin, K.G. Reid, B. Maiti, S.A. Ajuria, *Applied Physics Letters* 66 (1995) 2882–2884.
- [48] D.L. Perry, A. Grint, *Fuel* 62 (1983) 1024–1033.
- [49] A. Freitag, J. Rodriguez, J. Larese, *MRS Proceedings* 590 (1999) 189.
- [50] R.A. Schoonheydt, J.H. Lunsford, *Journal of Catalysis* 26 (1972) 261–271.